Improvement of Transient Voltage Responses using an Additional PID-loop on ANFIS-based Composite Controller-SVC (CC-SVC) to Control Chaos and Voltage Collapse in Power Systems

by I Made Ginarsa

Submission date: 18-Nov-2022 12:15PM (UTC+0700)
Submission ID: 1957516214
File name: B_Vol.131_No.10_pp.836-848.pdf (1.27M)
Word count: 11670
Character count: 53773

電気学会論文誌 B（電力・エネルギー部門誌）
IEEJ Transactions on Power and Energy
Vol.131 No.10 pp.836–848 DOI: 10.1541/ieejpes.131.836

Paper

Improvement of Transient Voltage Responses using an Additional PID-loop on ANFIS-based Composite Controller-SVC (CC-SVC) to Control Chaos and Voltage Collapse in Power Systems

I Made Ginarsa[*,**,***] Student Member,
Mauridhi Hery Purnomo[**] Non-member,
Takashi Hiyama[***] Member
Adi Soeprijanto[**] Non-member
Syafaruddin[***] Non-member

(Manuscript received Jan. 18, 2011, revised May 19, 2011)

Chaos and voltage collapse are qualitative behaviors in power systems that exist due to lack of reactive power in critical loading. These phenomena are deeply explored using both detailed and approximate models in this paper. The ANFIS-based CC-SVC with an additional PID-loop was proposed to control these problems and to improve transient response of the detailed model. The main function of the PID-loop was to increase the minimum voltage and to decrease the settling time at transient response. The ANFIS-based method was chosen because its computational complexity was more efficient than Mamdani fuzzy logic controller. Therefore the convergence of training processes was more rapidly achieved by the ANFIS-based method. The load voltage was held to the setting value by adjusting the SVC susceptance properly. From the experimental results, the PID-loop was an effective controller which achieved good simulation result for the reactive load, the minimum voltage increased and the settling time decreased at the values of $j0.12$ pu, 0.9435 pu and 7.01 s, respectively.

Keywords: transient voltage, chaos, voltage collapse, power system control, ANFIS, PID-loop

1. Introduction

Load demand in a modern power system has grown up rapidly in recent year. However, the increment of power plants and transmission lines being built are very slow due to economical and environmental reasons. This situation will make the systems operate in critical mode at the boundary of stability region. Chaos and voltage collapse are nonlinear phenomena that exist in power systems with critical (heavy) loading condition. Chiang et al.[(1)] developed the voltage collapse model and described both the physical explanation and computational consideration of this problem. Static and dynamic models were used to know the detailed type of voltage collapse, wherein the static model was used before a saddle-node bifurcation, while the dynamic model was employed after the bifurcation[(1)(2)]. Meanwhile, the Lyapunov exponent which measured how rapidly the two nearby trajectories separate from one to another within the state space and broadband spectrum was used to confirm this observation[(3)]. Within the range of loading conditions, the sensitivity of chaotic behavior made power systems unpredictable after a finite time. In addition, within this range the effectiveness of any control scheme was questionable and should be reevaluated based on state vector information. Furthermore, nonlinear phenomena, including bifurcation, chaos and voltage collapse occurred in a power system model. The presence of various nonlinear phenomena was found to be a crucial factor in the inception of voltage collapse in this model[(4)(5)]. The problems of controlled and suppressed of the presence of nonlinear phenomena in the power systems were addressed in this paper. The bifurcation control approach modified its bifurcation according to the system state equations and controlled chaos in a power system model[(4)–(7)]. The presence of chaotic oscillations in a power system causing seriously unstable problem was studied by Yu et al. and Rajesh and Padiyar[(8)–(10)]. The existence of chaotic oscillations in power systems due to disturbing of energy (DE) at the rotor speed has been found in Ref. (11). In addition, the modeling of chaotic behavior using recurrent neural networks in power systems was previously studied in Ref. (12). Practical techniques for recognizing and classifying chaotic behavior were identified by Parker and Chua[(13)], while control and anti-control chaos were developed by Chen[(14)]. One scheme of chaos utility was used on electrical systems for smelting which was based on chaos control. Lei et al. demonstrated that chaotic steel-smelting ovens regulated their heating currents according to chaos control theory[(15)]. A control system using a neural-network controller was presumed to be able to stabilize the unstable focus points of 2-dimensional chaotic systems; although, Konishi and Kokame stated that the control system

* Dept. of Electrical Engineering, Mataram University
Jln. Majapahit No.62 Mataram, NTB, 83126 Indonesia
** Power System Simulation Laboratory, Dept. of Electrical Engineering, ITS
Kampus ITS Sukolilo, Surabaya, 60111 Indonesia
*** Dept. of Computer Science and Electrical Engineering, Kumamoto University
2-39-1, Kurokami, Kumamoto 860-8555, Japan

did not require this presumption [16].

A fuzzy logic controller (FLC) has been successfully applied to control and stabilize chaotic systems, such as the Lorenz system [17] and the Chua circuit [18]. Various studies on controlling transient chaos have been carried out, such as those by Dhamala et al., and Dhamala and Lai attempted to control transient chaos in power systems using a data time-series [19][20]. Strategies for controlling chaos in process plants have been tested on the discrete Henon map chaotic system [21].

A composite controller (CC) that has successfully controlled and suppressed chaos in power systems was reported in Refs. (4), (5). A nonlinear autoregressive moving average neural networks-based CC (NARMA-based CC) has been applied to control and suppress chaos and voltage collapse in power system model [22].

Static var compensator (SVC) placement is an attractive topic of research in power system engineering. There have been many methods applying the SVC placement optimally to maintain voltage stability, such as normal form analysis [23], multi-restart bender decomposition [24], reactive power spot price index (QSPI) [25] and genetic algorithms (GA) [26]. An SVC supplementary controller has been applied to improve the damping of inter-area oscillations in small signal stability [27].

Adaptive neuro-fuzzy inference systems (ANFIS) technology is a combination of neural networks and fuzzy inference systems. This technology has been applied on many engineering systems, including on the detection of inter-turn insulation and bearing wear faults in induction motors [28], as well as on supplementary controllers for damping low frequency oscillations in power systems [29] and automatic voltage regulators for generator systems [30]. An ANFIS-based CC has been successfully applied to control chaos in power systems [31]. Furthermore, an ANFIS-based CC-SVC has been used to control chaos, voltage collapse and control of reactive power in order to maintain the load voltage in power system operation [32]. Meanwhile, a PID controller has been proposed in practical engineering such as: a design method for fuzzy PID controller using modified triangular membership functions to improve system performance [33], a fuzzy PID controller using a novel particle swarm optimization-evolutionary programming-based (PSO-EP-based) hybrid algorithm [34], and an intelligent particle swarm optimized fuzzy PID controller for AVR system [35], while ANFIS-based CC-PID has been used to improve transient voltage responses in power systems [36].

In this paper, we focus on improvement of transient voltage responses using additional PID-loop on ANFIS-based CC-SVC to control chaos and voltage collapse in power systems. The PID controller was chosen because it was simple and easy to be implemented. Whilst, the ANFIS method was used in this research because its computational complexity was more effective than Mamdani fuzzy inference system. And, controller parameters were automatically updated by off-line training.

This paper is organized as follows: the detailed and approximate models of power systems are explained in Section 2. Qualitative behavior of power systems in critical mode is described in Section 3. Next, the ANFIS-based CC-SVC with an additional PID-loop design is depicted in Section 4. The simulation results and analysis are presented in Section 5. Finally, the conclusion is provided in the last section.

2. Power System Model

A synchronous machine was modeled as a voltage (E'_{q0}) behind a direct reactance (x'_d). The voltage magnitude was assumed as remaining constant at the pre-disturbance value. De Mello and Concordia, as well as Kundur derived this model of a machine connected to an infinite bus [37]. Meanwhile, if saturation and the stator resistance were neglected, the system's condition was balanced with a static load. The machine was connected to the infinite bus and supplied the load. Then the armature current flowed from the machine to the load. This current caused electrical torque on the stator winding, and vice versa. The mechanical torque was produced by the flux through the rotor winding. Meanwhile, when the rotor speed was constant, the rotor speed followed the synchronous speed. When there was imbalanced energy, the rotor speed accelerated or decelerated, which can be expressed by the following equation

$$\dot{\omega}_m = \frac{1}{M}\left(T_m - T_e - D\omega_m\right) \quad \cdots\cdots (1)$$

where T_m, T_e, ω_m, D and M are the mechanical torque, electrical torque, rotor speed, damping constant and inertia constant, respectively.

2.1 Detailed Model This system model was developed from the work of Chiang et al. [1], as shown in Fig. 1. This model represents the system as one synchronous machine that supplies power to a local dynamic load with a shunt capacitor (Bus 2) connected by a weak tie line to an external system (Bus 3). All parameter values are conveyed to Eqs. (2)–(4):

$$V'_0 = \frac{V_0}{\left(1 + C^2Y_0^{-2} - 2CY_0^{-1}\cos(\theta_0)\right)^{0.5}} \quad \cdots\cdots (2)$$

$$Y'_0 = Y_0\left(1 + C^2Y_0^{-2} - 2CY_0^{-1}\cos(\theta_0)\right)^{0.5} \quad \cdots\cdots (3)$$

$$\theta'_0 = \theta_0 + \arctan\left(\frac{CY_0^{-1}\sin(\theta_0)}{1 - CY_0^{-1}\cos(\theta_0)}\right) \quad \cdots\cdots (4)$$

By using the variables and parameters on Table 1, the V'_0, Y'_0, θ'_0 were obtained as follows: $V'_0 = 2.5$ pu, $Y'_0 = 8.0$ pu, $\theta'_0 = -0.209$ rad. Thus, power system equations are defined as follows:

$$\dot{\delta}_m = \omega_m \quad \cdots\cdots (5)$$

$$\dot{\omega}_m = \frac{1}{M}\Big[-D\omega_m + P_m + V_m{}^2Y_m\sin(\theta_m) + V_mV_LY_m\sin(\delta_L - \delta_m - \theta_m)\Big] \quad \cdots\cdots (6)$$

$$\dot{\delta}_L = \frac{1}{K_{q\omega}}\Big[-K_{qv}V_L - K_{qv2}V_L^2 + Q - Q_0 - Q_{1d}\Big] \quad \cdots\cdots (7)$$

$$\dot{V}_L = \frac{1}{TK_{q\omega}K_{pv}}\Big[K_{p\omega}K_{qv2}V_L^2 + (K_{p\omega}K_{qv} - K_{q\omega}K_{pv})V_L + K_{p\omega}(Q_0 + Q_{1d} - Q) - K_{q\omega}(P_0 + P_{1d} - P) + u(\omega_m)\Big] \quad \cdots\cdots (8)$$

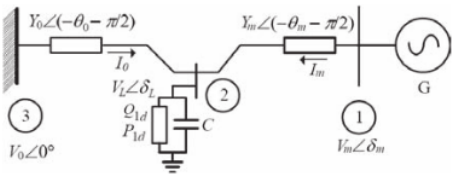

Fig. 1. Three-bus power systems

Table 1. Power system parameter values

Y_0	Y_m	V_0	V_m	θ_0	θ_m	P_m	M	D
20.0	5.0	1.0	1.0	−5.0	−5.0	1.0	0.3	0.05
$K_{p\omega}$	K_{pe}	$K_{q\omega}$	K_{qe}	K_{qe2}	C	P_0	Q_0	T
0.4	0.3	−0.03	−2.8	2.1	12.0	0.6	1.3	8.5

All parameter values are in pu except for angles, which are in degs

where the variables δ_m, ω_m, δ_L, V_L, P and Q are the power angle, rotor speed, angle, magnitude of the voltage at the load bus, real power and reactive power, respectively. The variables P and Q are computed using Eq. (9) and Eq. (10), respectively. The parameters P_{1d}, Q_{1d} and D are the real load, reactive load and damping constant. In this case, the parameter $u(\omega_m)$ was implemented as a control signal of the power systems.

$$P = -V_0' V_L Y_0' \sin(\delta_L + \theta_0') - V_m V_L Y_m \sin(\delta_L - \delta_m + \theta_m) + \left[Y_0' \sin(\theta_0') + Y_m \sin(\theta_m)\right] V_L^2 \quad \cdots\cdots (9)$$

$$Q = V_0' V_L Y_0' \cos(\delta_L + \theta_0') + V_m V_L Y_m \cos(\delta_L - \delta_m + \theta_m) - \left[Y_0' \cos(\theta_0') + Y_m \cos(\theta_m)\right] V_L^2 \quad \cdots\cdots (10)$$

2.2 Approximate Model An approximate which is a simplification of the detailed model with all the parameter values in Table 1 was fed to Eqs. (2)–(10). The approximate model is expressed as follows:

$$\dot{\delta_m} = \omega_m \quad \cdots\cdots (11)$$

$$\dot{\omega_m} = 16.667 \sin(\delta_L - \delta_m + 0.087) V_L - 0.1667\omega_m + 1.881 \quad \cdots\cdots (12)$$

$$\dot{\delta_L} = 496.872\, V_L^2 - \cos(\delta_L - \delta_m + 0.087) V_L - 666.667 \cos(\delta_L - 0.209) V_L - 93.333 V_L - 33.333 Q_{1d} + 43.333 \quad \cdots\cdots (13)$$

$$\dot{V_L} = -78.764\, V_L^2 + 104.869 \cos(\delta_L - 0.135) + 26.217 \cos(\delta_L - \delta_m - 0.012) V_L + 14.523\, V_L - 5.229 Q_{1d} - 7.033 \quad \cdots\cdots (14)$$

where the variables δ_m, ω_m, δ_L and V_L are the power angle, rotor speed, angle and magnitude of the voltage at the load bus, respectively. The parameter Q_{1d} is the reactive (inductive) load at load bus.

3. Qualitative Behavior of Power Systems in Critical Mode

Power systems are large dynamical systems with many nonlinearities. Thus it is quite possible that power systems qualitatively have rich behaviors due to sensitivity to tiny variation of initial conditions and parameters [3)–(5) (8)–(12)(32)(38)]. There were five types of qualitative behaviors observed and identified in power system operation in this study such as: Equilibrium point (EP), chaos, chaos to equilibrium point (CEP), chaos to voltage collapse (CVC) and voltage collapse (VC), which are listed in Table 2.

Table 2. Qualitative behaviors of power systems due to initial condition and parameter changes

DE(ω_0) [rad/s]	Reactive load (λ_0) [pu]	Qual. bhv.	Time [s]	Phase-plane trajectory
Detailed model: $\delta_{m0} = 0.2$ rad; $\delta_{L0} = 0.2$ rad; $V_{L0} = 0.98$ pu				
0.5	j10.894	EP	1,050	-
1.384	j10.894227220205999	CVC	2,803.2863	-
1.384	j10.8942272202059997	CEP	4,100	Figs. 2(a), (c)
1.384	j10.8942272202060009	CVC	8,292.6794	-
1.384	j10.894227220205	Chaos	∞	Fig. 3(a)
1.384	j10.89422822	CVC	410.3102	Fig. 3(c)
1.384	j10.896	VC	58.7401	-
1.396	j10.8906204	Chaos	∞	-
1.596	j10.8906204	Chaos	∞	-
1.68027	j10.8906204	Chaos	∞	-
1.68028	j10.8906204	VC	1.1281	-
Approximate model: $\delta_{m0} = 0.3$ rad; $\delta_{L0} = 0.3$ rad; $V_{L0} = 0.97$ pu				
0.5	j10.906201	EP	1,270	-
1.3824	j10.906201	CEP	2,780	Figs. 2(b), (d)
1.3824	j10.9062009	Chaos	∞	Fig. 3(b)
1.3824	j10.90622	CVC	1,074.4254	Fig. 3(d)
1.3824	j10.9069	VC	60.6985	-
1.5975	j10.9061	Chaos	∞	-
1.60584	j10.9061	Chaos	∞	-
1.65160	j10.9061	Chaos	∞	-
1.65161	j10.9061	VC	0.9772	-
EP: Equilibrium point		CEP: Chaos to equilibrium point		
VC: Voltage collapse		CVC: Chaos to voltage collapse		

The balancing of reactive power is very important to keep voltage stability in power system operation. When the power systems work under low reactive power supporting, the systems will operate under-voltage condition. Furthermore, voltage collapse will occur if the systems operate under lack of the reactive power. But, when a low reactive power demand and the reactive power excess in the systems, the power systems will operate on over-voltage condition. Over-voltage causes insulation deterioration and device damage.

Disturbing of energy (DE) was used as an initial condition because the DE corresponded to real power in power systems. When electrical and mechanical power in a generator were balanced, the power systems operated in normal condition. But, when a large load shedding occurred, the excess of its mechanical power was identified as the DE.

3.1 Chaos to Equilibrium Point Due to Reactive Load Change The CEP with 2 circles is the qualitative behavior with exotic phenomena obtained in the δ_L-V_L phase-plane. The CEP occurred in the detailed model when the initial conditions were at the values of [0.2 1.384 0.2 0.98] and the parameter (reactive load, λ_0) was at the value of j10.8942272202059997 pu. Based on Table 2, chaos to voltage collapse (CVC) occurred before the CEP phenomenon. The CVC for the reactive load and time of this occurrence was at the values of j10.894227220205999 pu and 2,803.2863 s, respectively. Furthermore, the reactive load was increased to j10.8942272202060009 pu, the CVC

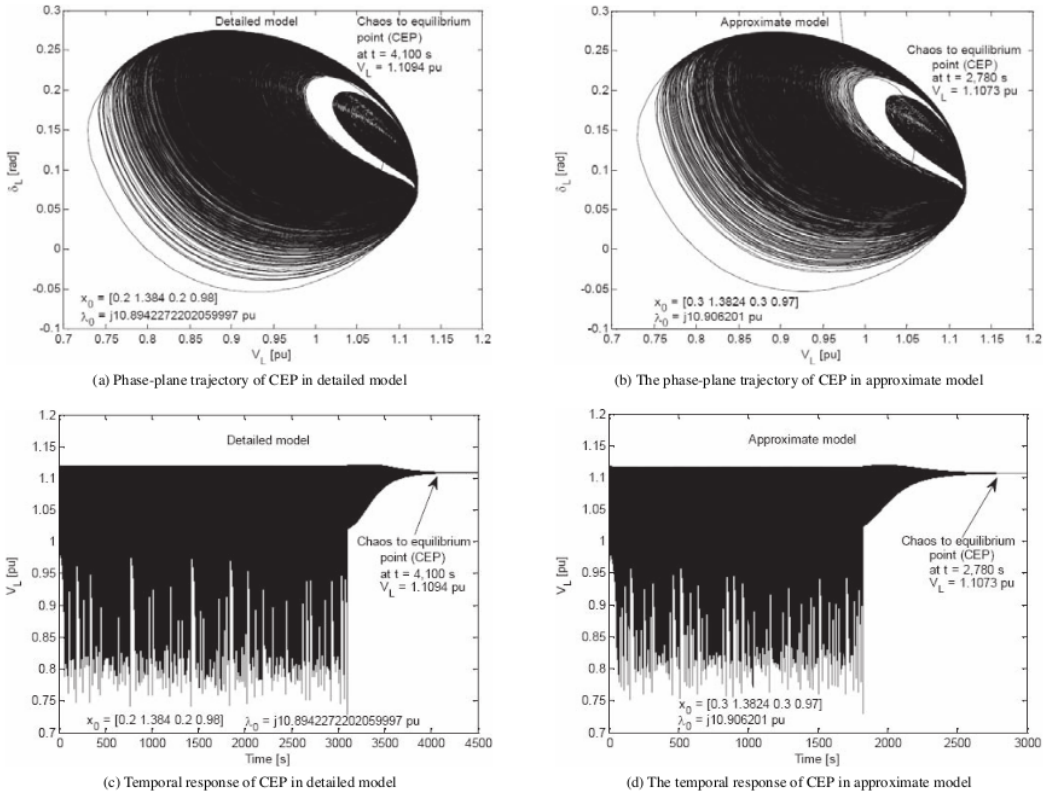

(a) Phase-plane trajectory of CEP in detailed model

(b) The phase-plane trajectory of CEP in approximate model

(c) Temporal response of CEP in detailed model

(d) The temporal response of CEP in approximate model

Fig. 2. The phase-plane trajectories and temporal responses of CEP in critical mode power systems

occurred again at time of 8,292.6794 s. It is shown that the CEP is very sensitive to the reactive load change. The CEP route trajectories of the δ_L-V_L phase-plane and V_L temporal response of the detailed model are shown in Fig. 2(a) and Fig. 2(c), respectively. It is shown that chaotic oscillation (transient chaos [20]) occurred from 0 to 3,000 s. Then the V_L trajectory converged to an equilibrium point at 4,100 s and the steady-state V_L at 1.1094 pu. Meanwhile, the approximate model exhibited the CEP phenomenon with the initial condition at [0.3 1.3824 0.3 0.97] and the reactive load (λ_0) at j10.906201 pu. The CEP occurred at time of 2,780 s and the V_L at 1.1073 pu. The δ_L-V_L phase-plane and V_L temporal response are shown in Fig. 2(b) and Fig. 2(d), respectively.

Intrinsically, power systems are nonlinear systems which consist of many nonlinearity components and devices. This is the same as chaos phenomenon appeared in nonlinear systems including power system simulation which have been reported in Refs. (3)–(5) (8)–(22). In this research, the CEP phenomenon also appeared in power system simulation when the parameter and initial condition of power systems were at exact values.

3.2 Other Qualitative Behaviors Due to Reactive Load Change Power systems produced other qualitative behaviors when they operated in critical loading. First, they took a longer to move in chaotic oscillation (chaos) when the λ_0 values for the detailed and approximate models were decreased to j10.894227220205 and j10.9062009 pu, respectively as shown in Fig. 3(a) and Fig. 3(b). Furthermore, when the λ_0 values was slightly increased to j10.89422822 and j10.90622 pu, CVC states occurred again. This occurrence made the V_L trajectories for the detailed and approximate model in transient chaos and finally collapse at times of 410.3102 and 1,074.4254 s as shown in Fig. 3(c) and Fig. 3(d). The dynamic fall of voltages in this transient was identified as a voltage collapse (VC) [39]. Based on Table 2, when the λ_0 values was increased to j10.896 and j10.9069 pu, power systems lost their equilibrium point and led to instability region. Several VC for the detailed and approximate models occurred in power systems at times of 58.7401 and 60.6985 s, respectively. Unfortunately, the illustrations of the VC temporal responses from detailed and approximate models are omitted here because of space limitation.

4. ANFIS-based CC-SVC with an Additional PID-loop Design

4.1 Composite Controller Design Two types of control law, namely linear controller and nonlinear (cubic) controller were combined to produce composite controller. The function of linear controller was to improve both static and dynamic stability margins. Meanwhile, the function of cubic controller was to avoid chaos, voltage collapse and to

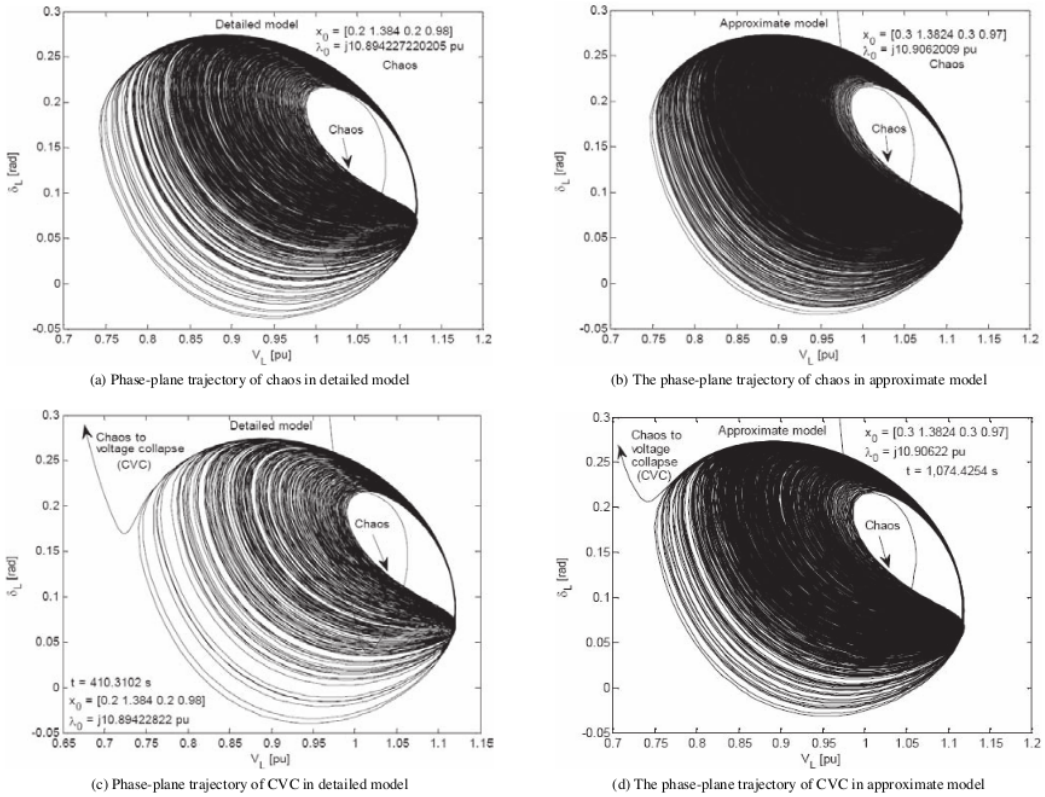

(a) Phase-plane trajectory of chaos in detailed model

(b) The phase-plane trajectory of chaos in approximate model

(c) Phase-plane trajectory of CVC in detailed model

(d) The phase-plane trajectory of CVC in approximate model

Fig. 3. The phase-plane trajectories of chaos and CVC in critical mode power systems

improve stability degree [4]. The formulation of linear and nonlinear feedback controller with measurement of ω_m and u, can be written as follows:

$$u = k_l \omega_m \quad \cdots\cdots (15)$$

$$u = k_n (\omega_m)^3 \quad \cdots\cdots (16)$$

Furthermore, composite controller can be expressed as a combination of linear and nonlinear feedback control. The closed loop of power system formulas are shown in Eqs. (5)–(8) with the ω_m and u can be expressed as the following equation

$$u = k_l \omega_m + k_n (\omega_m)^3 \quad \cdots\cdots (17)$$

where the variable ω_m is the rotor speed, and the parameters u, k_l, k_n are the control signal, linear gain, and nonlinear gain, respectively.

4.2 PID Controller Design PID controllers have been extensively used by industries due to their simple structure, which can be easily understood and implemented. Our main focus was to eliminate steady state error as well as to improve the dynamic response. The elimination of steady state error could be realized by adding a pole at the origin using an integral controller, while transient response improvement was achieved by the action of differential controller. As modeled in this paper, the transfer function of PID controller [35] is expressed as follows:

$$G(s) = k_p + \frac{k_i}{s} + k_d s \quad \cdots\cdots (18)$$

where $G(s)$, k_p, k_i, k_d and s are the transfer function, proportional gain, integral gain, differential gain and Laplace operator, respectively. Block diagram of the CC-PID controller is shown in Fig. 4(a).

4.3 SVC Controller Design Let us start with SVC that was applied at bus k, and the reactive power was injected to bus k

$$Q_k = V_k^2 B_{SVC} \quad \cdots\cdots (19)$$

where $B_{SVC} = B_C - B_L$, B_{SVC}, B_C and B_L are the SVC, capacitive and inductive susceptances, respectively. Dynamic equations of SVC can be written as follows [40]:

$$\Delta \dot{B}_{SVC} = \frac{1}{T_{SVC}} \left[\left(1 - \frac{T_{v1}}{T_{v2}} \right) \Delta V_{r-SVC} - \Delta B_{SVC} - \frac{K_v T_{v1}}{T_{v2}} \Delta V_{t-SVC} \right] + \frac{K_v T_{v1}}{T_{v2} T_{SVC}} \left[\Delta V_{ss-SVC} + \Delta V_{ref} \right] \cdots\cdots (20)$$

where T_{SVC}, T_{v1}, T_{v2}, K_v, ΔV_{ss-SVC}, ΔV_{r-SVC}, ΔV_{t-SVC} and ΔV_{ref} are the SVC time constant, time constant 1, time

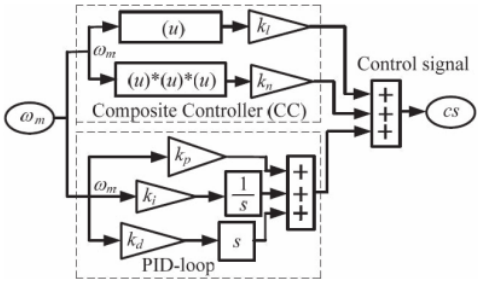

(a) Block diagram of CC-PID

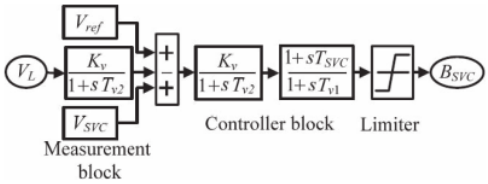

(b) Block diagram of SVC device

Fig. 4. Conventional forms of proposed controller

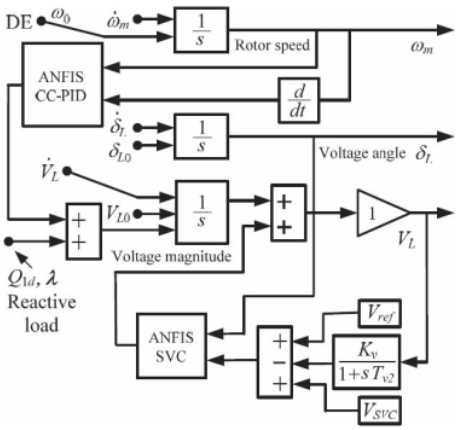

Fig. 5. The proposed controller was applied to power systems

constant 2, SVC gain, SVC voltage at steady state, difference of reference and SVC voltage, difference of terminal and SVC voltage and reference voltage, respectively. And parameter values of SVC for the T_{SVC}, T_{v1}, T_{t2} and K_{v_SVC} were 70.0, 3.0729 – 117.96, 400.0 and 30.0, respectively. Block diagram of the SVC is shown in Fig. 4(b). Meanwhile, block diagram of the proposed controller applied to power systems is shown in Fig. 5.

4.4 ANFIS Design Processes A Detailed method of ANFIS-based CC-SVC with an additional PID-loop design is presented as follows:

(1) Selection of input variables: In this step, the state variables provided as input signals to the controller were chosen.

(a) The rotor speed (ω_m) and its derivative ($\dot{\omega}_m$) for the ANFIS-based CC-PID.

(b) The voltage angle (δ_L) and voltage magnitude (V_L) for the ANFIS-based SVC.

(2) Selection of linguistic variables: Five linguistic variables were used to describe each of the input variables.

(a) Negative high (NH), negative low (NL), zero (ZE), positive low (PL) and positive high (PH) for the CC-PID.

(b) Small (SM), low to medium (LM), medium (MD), medium to high (MH) and high (HI) for the SVC.

(3) Selection of membership functions: Gaussian membership functions were used to define the degree of membership of input variables. A Gaussian membership function was specified by two parameters (c, σ), where c and σ represent the membership function center and width (spread), respectively. These parameters were obtained automatically through learning processes by a hybrid algorithm[41][42].

(4) Selection of fuzzy model: A first-order fuzzy model Sugeno (T-S) was chosen in this design because of its computational efficiency.

(5) Preparation of training data pairs: There were two sets of data training pairs:

(a) The rotor speed (ω_m), its derivative ($\dot{\omega}_m$) and control signal (cs) as the 2 inputs and output of the ANFIS-based CC-PID, respectively.

(b) The voltage angle (δ_L), voltage magnitude (V_L) and SVC susceptance (B_{SVC}) as the 2 inputs and output of the ANFIS-based SVC, respectively.

(6) Optimization of unknown parameters: The unknown parameters of the Gaussian membership function, such as center, spread and the linear output of each rule of the first-order Sugeno fuzzy model were optimized by using a matrix of training data pairs. All initial values for the center and the spread of each input membership function were assumed as zero for each rule. Furthermore, the input and output parameters were optimized using the back-propagation algorithm and the least squares estimation (LSE) method, respectively.

4.5 Training Process of ANFIS-based Controller Parameters The training processes were performed using off-line methods with 6,000 data points. The training of data pairs were prepared by simulating power systems with a conventional CC and additional PID-loop (CC-PID-SVC). By this training, the values for the number of nodes, linear parameters, nonlinear parameters and fuzzy rules were obtained at 75, 75, 20 and 25, respectively. Each input parameter was represented by 5 Gaussian membership functions. The input-output control surface views of the ANFIS-based CC-PID and SVC of additional reactive load at $j0.12$ pu are shown in Fig. 6(a) and Fig. 6(b), respectively.

Figure 6(a) shows the nonlinear relationship of 2 inputs (ω; $\dot{\omega}$) and an output (cs) with 2 hills (maximum values) and 2 valleys (minimum values). The first hill was achieved at 0.19 when the inputs for the rotor speed and its derivative were at 0.05 rad/s and 1.0 rad/s^2, respectively. The control signal (cs) in this case did not have any dimension unit. Meanwhile,

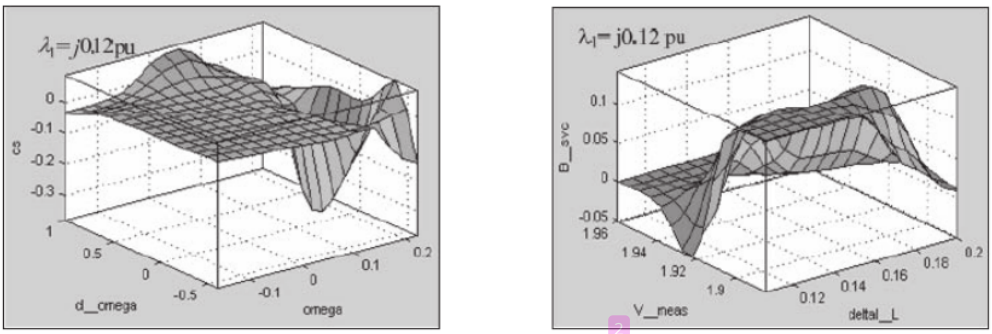

(a) Input-output control surface of ANFIS-based CC-PID (b) Input-output control surface of ANFIS-based SVC

Fig. 6. Control surface of the proposed controller

second hill was achieved at the value of 0.1 when the inputs for rotor speed and its derivative were at the values of 0.205 rad/s and −0.45 rad/s^2, respectively. In contrast, the first valley was achieved at −0.37 when the inputs for the rotor speed and its derivative were at the values of 0.18 rad/s and 0.15 rad/s^2. And the second valley was achieved at the value of −0.23 when the inputs for the rotor speed and its derivative were at the values of 0.22 rad/s and 0.52 rad/s^2, respectively.

Figure 6(b) shows the nonlinear relationship of voltage angle (δ_L) as an input 1 and voltage measurement as an input 2 (V_m) and SVC susceptance as an output (B_{SVC}). The surface of SVC susceptance sharply increased with the hill (maximum value) at 0.141 pu. This value was achieved when the voltage angle was from 0.11 to 0.16 rad and the voltage measurement was from 1.86 to 1.90 pu. The valley (minimum value) was achieved at −0.05 pu when the voltage angle was at the value of 0.11 rad and the voltage measurement was from 1.921 to 1.929 pu.

5. Simulation Results and Analysis

The performance of the proposed controller was illustrated and tested considering a high load in power systems. Simulation results were obtained by Matlab/Simulink V.7.6.0 324 on an Intel Core 2 Duo E6550 @ 2.33 GHz PC computer. The simulations were done as follows:

(1) The DE and additional reactive load (λ_0) were forced to power systems with the detailed and approximate models. The responses of the systems are presented in Table 2 and Figs. 2(a)–3(d).

(2) In this research, the detailed model power system was chosen to be implemented with the proposed controller because its responses were better than the others. Its model was able to give settling time responses less than 20 s. In addition, the detailed model was able to cover the DE and reactive load at values of 1.35 rad/s and j0.20 pu, respectively. Meanwhile, the settling time of the approximate model responses were more than 30 s. Its model ability was limited for the additional DE and reactive load at the values of 0.5 rad/s and j0.02 pu, respectively.

(3) The ANFIS-based CC-SVC with an additional PID-loop was proposed to improve the transient voltage magnitude responses in power system model. The proposed controller was compared with other methods in order to validate simulation result. In this test, 2 scenarios were taken and illustrated as follows:

(a) Scenario 1: Several DE were added to the rotor speed at the generator bus in 4 stages: 1.2744, 1.30, 1.325 and 1.35 rad/s. The simulation results are presented in Table 3, Fig. 7(a) and Fig. 7(b).

(b) Scenario 2: The reactive (j0.0 to j0.20 pu), real (0.02 to 0.22 pu) and complex (0.0 + j0.0 to 0.17 + j0.17 pu) loads were added to the load bus. The simulation results are presented in Tables 4, 5 and Figs. 8(a)–11.

5.1 Power Systems without Control Device Power systems without any control system are very vulnerable to disturbances during operation under critical (heavy) loading. From Table 2, we can see that the power systems without any controller only covered limited load at 0.6+j10.896 pu. On the other hand, a power system equipped by controller was adequate to cover initial load at 0.6+j11.27 pu. Moreover, this system was also adequate to cover the additional reactive, real and complex loads at j0.2, 0.22 and 0.17+j0.17 pu, respectively. The ability of respective controller will be explored in the following sub-section.

In this research, disturbances which were forced into power systems were the DE and reactive load as initial conditions and parameters, respectively. The qualitative behavior of power systems spontaneously changed when the initial condition, parameter or both of them were changed. Both the DE and reactive load were increased step by step and the phase-plane trajectories and time responses of power systems were observed and identified. Meanwhile, the EP with a longer time oscillation had to be avoided by means of a control scheme. On the other hand, the CEP, chaos, CVC and VC phenomena were unwanted qualitative behaviors because all of phenomena led power systems to lose stability. When they exist in power systems, the operator must anticipate these phenomena using some control schemes immediately.

5.2 Power Systems with the LC-SVC or ANFIS-based CC-SVC Power systems were equipped by a Linear Controller-SVC (LC-SVC) or an ANFIS-based CC-SVC to control voltage magnitude to the desired level. Both controllers were adequate to control chaos and voltage collapse of power system operation. However, performances of the respective controllers were not good enough. The load voltage

Table 3. Simulation results of the proposed controller with various DE

DE	Conventional CC				LC-SVC			ANFIS-based CC-SVC			Proposed controller		
	V_{min}	t_{min}	t_{st}	t_{ON}	V_{min}	t_{min}	t_{st}	V_{min}	t_{min}	t_{st}	V_{min}	t_{min}	t_{st}
[rad/s]	[pu]	[s]	[s]	[s]	[pu]	[s]	[s]	[pu]	[s]	[s]	[pu]	[s]	[s]
1.2744	0.927	0.50	5.25	1.92	0.926	2.37	9.21	0.848	2.51	6.12	0.932	2.34	5.10
1.30	0.916	0.52	5.31	2.5	0.963	2.43	9.54	0.853	2.58	6.15	0.965	2.98	5.11
1.325	0.896	0.53	6.04	3.0	0.927	2.74	10.04	0.857	3.54	6.16	0.952	2.51	5.12
1.35	0.895	0.56	6.25	3.4	0.933	4.0	11.46	0.865	4.01	6.17	0.950	2.58	5.14

V_L:convent. CC = 1.086 pu; $B_{SVC} = -j0.4063$ pu; $Q_{SVC} = -j0.4013$ pu; V_L:other contrs. = 0.98 pu

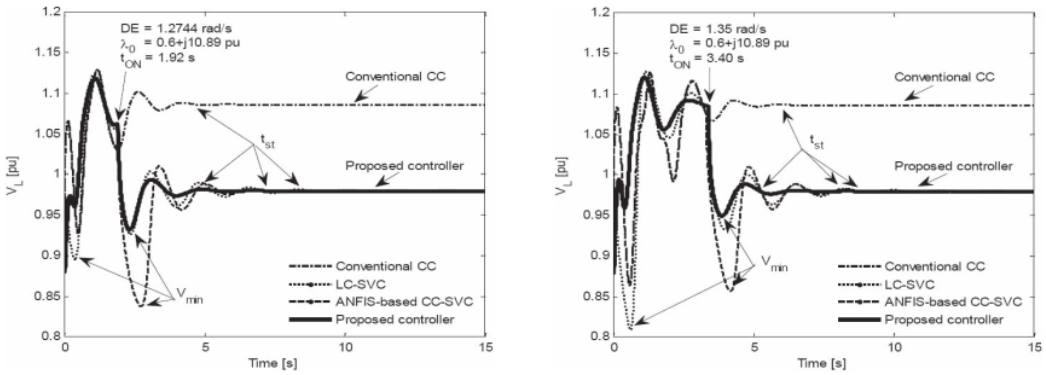

(a) DE = 1.2744 rad/s (b) DE = 1.35 rad/s

Fig. 7. Performance of respective controllers with several additional DE were forced to power systems

(V_L) temporal response still fluctuated in few seconds. Furthermore, the first swing minimum voltage (minimum voltage, V_{min}) was too low. Consequently, the power systems tended to enter the unstable region or voltage collapse occurred.

The V_L temporal responses for an additional reactive load at the value of $j0.12$ pu are as follows: the minimum voltages for LC-SVC and ANFIS-based CC-SVC were obtained at the values of 0.9246 and 0.9362 pu, respectively and the settling times were obtained at 16.27 and 12.05 s. The V_L temporal responses of these controllers are shown in Fig. 9.

5.3 Power Systems with the Proposed Controller

The proposed controller was used to improve the transient voltage responses at critical loading. Both chaos and voltage collapse were controlled and suppressed using a combination of an ANFIS-based CC-PID and SVC devices. Parameter values of the CC for k_l and k_n were taken at 0.08 and 0.08, respectively. The main function of an additional PID-loop was to improve transient voltage responses through increasing the minimum voltage and decreasing the settling time. Parameter values of the PID-loop for the k_p, k_i and k_d were taken at 2.1995×10^{-2}, 3.9439×10^{-4} and 8.3×10^{-3}, respectively. The main function of the SVC device was to regulate the load voltage through controlling the susceptance properly. The reactive power was absorbed by the SVC device from the networks when the load voltage was at high level value. On the contrary, the reactive power was supplied to the networks when the load voltage was at a low level value due to critical (heavy) loading.

5.3.1 Scenario 1: Controller performance at additional DE Power systems were forced by the DE into the rotor speed. The DE was increased in 4 steps with the values of 1.2744, 1.30, 1.325 and 1.35 rad/s. Next, the SVC ON adjustment time (t_{ON}) was also increased at the values of 1.92, 2.5, 3.0 and 3.4 s. These results are listed in Table 3.

Figure 7(a) shows that the V_L temporal responses were able to be controlled on a fixed point ($V_L = 0.98$ pu) when the SVC device was applied to power systems. The response of power systems was obtained by simulating DE, reactive load and t_{ON} at the values of 1.2744 rad/s, $j10.89$ pu and 1.92 s, respectively. Fig. 7(a) shows that the V_L temporal responses of respective controller were then compared to others in order to validate the simulation results.

From the Fig. 7(a) and Table 3, we can see that the V_L temporal response of the conventional CC for the minimum voltage (V_{min}), time of minimum voltage(t_{min}) and settling time (t_{st}) was obtained at the values of 0.927 pu, 0.5 s and 5.25 s, respectively. However, the steady state V_L was still uncontrolled at 1.086 pu (This value is higher than a reference voltage ($V_{ref} = 0.98$ pu)). On the contrary, when systems were equipped by LC-SVC, the V_L temporal response for the V_{min}, t_{min} and t_{st} were obtained at the values of 0.926 pu, 2.37 s and 9.21 s, respectively. The V_L temporal response of power systems, when equipped by an ANFIS-based CC-SVC for the V_{min}, t_{min} and t_{st}, was obtained at the values of 0.848 pu, 2.51 s and 6.12 s, respectively. Moreover, when the CC-SVC with an additional PID-loop was applied to power systems, the V_L temporal response was improved significantly at the values of 0.932 pu, 2.34 s and 5.10 s for the V_{min}, t_{min} and t_{st}, respectively.

The V_L temporal responses in which the DE was forced to rotor speed at the value of 1.35 rad/s and t_{ON} at the value of 3.4 s are shown in Fig. 7(b). When the DE was increased, the stress on the power systems also increased. It was more

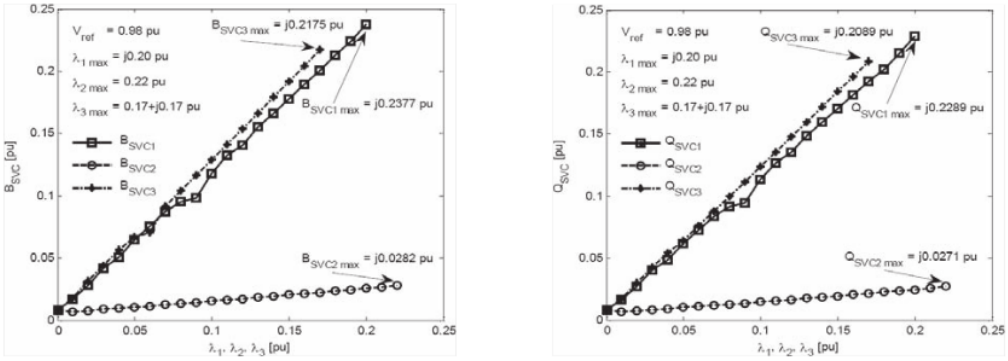

(a) Susceptance of SVC (B_{SVC}) (b) Reactive power was supplied by the SVC (Q_{SVC})

Fig. 8. Graphs of B_{SVC} and Q_{SVC} when λ_1, λ_2 and λ_3 were increased and V_{ref} at 0.98 pu

difficult to reduce this disturbance rapidly. Consequently, voltage collapse occurred if the load voltage decreased too early. In order to avoid this voltage collapse, proper SVC ON adjustment time (t_{ON}) must be realized.

From Fig. 7(b) and Table 3, it can be seen that the V_L temporal responses for the V_{min}, t_{min} and t_{st} were obtained at the values of 0.895 pu, 0.56 s and 6.25 s, respectively when a conventional CC was applied to power systems. Meanwhile, the V_L temporal response of power systems equipped by LC-SVC produced the values for the V_{min}, t_{min} and t_{st} as follows: 0.933 pu, 4.0 s and 11.46 s, respectively. The V_L temporal response of system with an ANFIS-based CC-SVC for the V_{min}, t_{min} and t_{st} was obtained at the values of 0.865 pu, 4.01 s and 6.17 s, respectively. Furthermore, when the proposed controller was applied to power systems, it was able to improve the V_L temporal response for the V_{min}, t_{min} and t_{st} with the values of 0.950 pu, 3.58 s and 5.14 s, respectively. The proposed controller was able to increase the minimum voltage and decrease the settling time by adjusting the nonlinear gain and the PID gain properly.

From scenario 1, it is found out that the V_L temporal response of the proposed controller gave the highest value of minimum voltage (V_{min}) and the shortest settling time (t_{min}). It means that the proposed controller gives a better response than the other 2 controllers. Performance of the proposed controller compared to the CC, LC-SVC and ANFIS-based CC-SVC in power systems can be described as follows. Firstly, a conventional CC was applied to power systems, then the chaos was suppressed and controlled by this method. The result was that the steady state V_L was obtained in a high value (V_L = 1.086 pu). From Fig. 7(a) and Fig. 7(b), we can see that the conventional CC was not able to control/maintain the voltage magnitude (V_L) because its controller did not have voltage controller device. Secondly, the V_L was able to be improved at the setting value of 0.98 pu when the SVC was applied to power systems. In this scenario, a reference voltage was kept at a fixed value (V_{ref} = 0.98 pu). By adjusting the SVC susceptance (B_{SVC}), reactive power absorbed by the SVC (Q_{SVC}) from the networks was controlled and the steady state V_L was able to reach the reference voltage. Therefore, simulation results for the B_{SVC}, Q_{SVC} and steady state V_L were obtained at the values of $-j0.4063$, $-j0.4013$ and 0.98 pu, respectively. From simulation results of the Scenario 1, performance of controllers has been clearly explained. The simulation results of this scenario show that all the controllers led the power systems not to be sensitive to disturbing of energy (DE). Unfortunately, these controllers just work on limited range at the DE 1.35 rad/s.

5.3.2 Scenario 2: Controller performance at additional load In the next scenario, performance of the proposed controller was evaluated by adding 3 types of loads such as: Reactive (λ_1), real (λ_2) and complex (λ_3) loads. Initial condition was taken at the value of $0.6 + j11.27$ pu. The reference voltage was given at a fixed value (V_{ref} = 0.98 pu). The B_{SVC}, Q_{SVC} and steady state V_L values were observed as the output data. The simulation results are listed in Table 4. Moreover, the V_L temporal responses were observed at the minimum voltage (V_{min}), time of minimum voltage (t_{min}) and settling time (t_{st}) are summarized in Table 5.

The values of B_{SVC} of the λ_1, λ_2 and λ_3 loads were obtained from $j0.0084$ to $j0.2377$, from $j0.0069$ to $j0.0282$ and from $j0.0181$ to $j0.2175$ pu, respectively. And, the values of Q_{SVC} of the λ_1, λ_2 and λ_3 were obtained from $j0.0081$ to $j0.2289$, from $j0.0067$ to $j0.0271$ and from $j0.0174$ to $j0.2089$ pu, respectively. At this setting, the maximum additional loads for the λ_1, λ_2 and λ_3 were handled at the values of $j0.20$, 0.22 and $0.17 + j0.17$ pu, respectively. The steady state values of V_L for the λ_1, λ_2 and λ_3 were obtained on the fixed point at 0.9814, 0.9801 and 0.9801 pu, respectively. The relations of the B_{SVC}, Q_{SVC}, V_L and error percentage against the λ_1, λ_2 and λ_3 values are listed in Table 4.

The graphs of the B_{SVC} and Q_{SVC} against 3 types of additional loads are shown in Figs. 8(a) and (b), respectively. Figures 8(a) and (b) show that the B_{SVC} and Q_{SVC} values of the λ_1 and λ_3 more rapidly increased than the B_{SVC} and Q_{SVC} values of the λ_2. It is shown that the change of reactive load led power systems operation to find out a new operating point in order to keep its stability.

Figures 8(a) and (b) prove that the reactive power in the networks was strongly connected to the B_{SVC} and Q_{SVC} on the voltage control scheme point of view. The B_{SVC} value needed to be increased in order to keep reactive power to support the networks and to maintain the load voltage at the setting value when the load in power systems increased.

Table 4. The B_{SVC} and Q_{SVC} for different load types and V_{ref} at the value of 0.98 pu

λ_1 [pu]	B_{SVC} $\times j$ [pu]	Q_{SVC} $\times j$ [pu]	V_L [pu]	Err [%]	λ_2 [pu]	B_{SVC} $\times j$ [pu]	Q_{SVC} $\times j$ [pu]	V_L [pu]	Err [%]	λ_3 [pu]	B_{SVC} $\times j$ [pu]	Q_{SVC} $\times j$ [pu]	V_L [pu]	Err [%]
j0.00	0.0084	0.0081	0.9800	0.00	0.01	0.0069	0.0067	0.9800	0.00	0.01+j0.01	0.0181	0.0174	0.9800	0.00
j0.02	0.0284	0.0272	0.9800	0.00	0.04	0.0097	0.0093	0.9800	0.00	0.02+j0.02	0.0317	0.0305	0.9801	0.01
j0.04	0.0509	0.0490	0.9800	0.00	0.06	0.0116	0.0112	0.9800	0.00	0.04+j0.04	0.0568	0.0546	0.9805	0.05
j0.06	0.0757	0.0727	0.9799	0.01	0.08	0.0136	0.0131	0.9800	0.00	0.06+j0.06	0.0792	0.0760	0.9800	0.00
j0.08	0.0958	0.0920	0.9800	0.00	0.10	0.0155	0.0149	0.9801	0.01	0.08+j0.08	0.1039	0.0998	0.9800	0.00
j0.10	0.1183	0.1137	0.9800	0.00	0.12	0.0175	0.0168	0.9800	0.00	0.10+j0.10	0.1287	0.1236	0.9800	0.00
j0.12	0.1410	0.1354	0.9800	0.00	0.14	0.0195	0.0187	0.9800	0.00	0.12+j0.12	0.1539	0.1478	0.9800	0.00
j0.14	0.1665	0.1599	0.9799	0.01	0.16	0.0215	0.0207	0.9799	0.01	0.13+j0.13	0.1666	0.1600	0.9800	0.00
j0.16	0.1893	0.1818	0.9800	0.01	0.17	0.0225	0.0216	0.9800	0.00	0.14+j0.14	0.1793	0.1722	0.9801	0.01
j0.17	0.2007	0.1928	0.9800	0.00	0.18	0.0236	0.0227	0.9800	0.00	0.15+j0.15	0.1919	0.1843	0.9800	0.00
j0.18	0.2133	0.2020	0.9800	0.00	0.20	0.0257	0.0247	0.9800	0.00	0.16+j0.16	0.2047	0.1966	0.9800	0.00
j0.20	0.2377	0.2289	0.9814	0.14	0.22	0.0282	0.0271	0.9801	0.01	0.17+j0.17	0.2175	0.2089	0.9801	0.01

Table 5. Performance of the controller at V_{ref} = 0.98 pu

λ [pu]	LC-SVC									ANFIS-based CC-SVC								
	λ_1			λ_2			λ_3			λ_1			λ_2			λ_3		
	V_{min} [pu]	t_{min} [s]	t_{st} [s]	V_{min} [pu]	t_{min} [s]	t_{st} [s]	V_{min} [pu]	t_{min} [s]	t_{st} [s]	V_{min} [pu]	t_{min} [s]	t_{st} [s]	V_{min} [pu]	t_{min} [s]	t_{st} [s]	V_{min} [pu]	t_{min} [s]	t_{st} [s]
0.00	0.9340	0.63	16.05	-	-	-	-	-	-	0.9207	0.59	11.05	-	-	-	-	-	-
0.02	0.9326	0.62	15.94	0.9441	0.60	18.72	0.9450	0.59	18.01	0.9180	0.61	11.12	0.9441	0.59	17.10	0.9485	0.67	16.94
0.04	0.9313	0.62	15.95	0.9444	0.59	18.02	0.9452	0.58	18.03	0.9386	0.56	12.04	0.9442	0.59	17.12	0.9488	0.65	16.95
0.06	0.9299	0.62	16.07	0.9446	0.59	18.08	0.9428	0.58	18.02	0.9127	0.63	12.22	0.9442	0.60	17.03	0.9455	0.63	17.12
0.08	0.9282	0.62	16.23	0.9449	0.59	18.12	0.9423	0.57	18.03	0.9048	0.67	12.84	0.9441	0.59	17.31	0.9449	0.61	17.10
0.10	0.9265	0.63	16.24	0.9451	0.59	18.72	0.9422	0.55	18.04	0.8963	0.72	12.76	0.9441	0.57	17.08	0.9453	0.60	17.98
0.12	0.9246	0.63	16.27	0.9453	0.59	18.11	0.9413	0.55	18.16	0.9362	0.69	12.05	0.9441	0.59	17.16	0.9436	0.59	17.02
0.14	0.9225	0.64	16.28	0.9454	0.58	18.09	0.9403	0.54	18.19	0.8929	0.76	12.27	0.9441	0.59	17.06	0.9438	0.57	16.67
0.16	0.9201	0.65	16.26	0.9460	0.55	18.21	0.9403	0.53	18.23	0.9365	0.60	12.83	0.9441	0.59	17.05	0.9438	0.57	16.88
0.17	0.9193	0.65	16.26	0.9460	0.55	18.22	0.9406	0.52	18.27	0.9236	0.60	13.96	0.9440	0.59	17.11	0.9394	0.52	17.02
0.18	0.9197	0.64	16.31	0.9460	0.55	18.20	-	-	-	0.9401	0.61	13.10	0.9440	0.59	17.10	-	-	-
0.20	0.9119	0.62	16.44	0.9461	0.54	18.15	-	-	-	0.8785	0.92	13.11	0.9440	0.59	17.09	-	-	-
0.22	-	-	-	0.9464	0.54	18.10	-	-	-	-	-	-	0.9440	0.59	17.12	-	-	-

λ [pu]	Proposed controller								
	λ_1			λ_2			λ_3		
	V_{min} [pu]	t_{min} [s]	t_{st} [s]	V_{min} [pu]	t_{min} [s]	t_{st} [s]	V_{min} [pu]	t_{min} [s]	t_{st} [s]
0.00	0.9660	0.51	7.56	-	-	-	-	-	-
0.02	0.9185	0.61	7.88	0.9383	0.49	11.81	0.9504	0.57	12.02
0.04	0.9172	0.60	7.51	0.9383	0.49	11.81	0.9450	0.60	12.61
0.06	0.9117	0.61	7.76	0.9383	0.49	11.81	0.9431	0.47	12.01
0.08	0.9427	0.38	7.86	0.9381	0.47	12.10	0.9410	0.53	11.67
0.10	0.9430	0.39	7.58	0.9380	0.45	12.45	0.9370	0.50	11.78
0.12	**0.9435**	**0.39**	**7.01**	0.9374	0.50	10.31	0.9407	0.53	11.70
0.14	0.9357	0.41	7.14	0.9370	0.48	10.52	0.9310	0.50	11.74
0.16	0.9316	0.41	7.25	0.9386	0.48	11.55	0.9420	0.54	12.34
0.17	0.9321	0.42	8.38	0.9387	0.48	11.57	0.9428	0.53	12.57
0.18	0.9323	0.42	9.03	0.9375	0.48	12.58	-	-	-
0.20	0.9326	0.42	9.14	0.9511	1.25	12.50	-	-	-
0.22	-	-	-	0.9624	1.26	12.53	-	-	-

λ_1: $j0.00 - j0.20$ pu
λ_2: $0.02 - 0.22$ pu
λ_3: $0.02 + j0.02 - 0.17 + j0.17$ pu

The Q_{SVC} was needed to maintain reactive power balance in power systems and to prevent voltage collapse occurrence under critical (heavy) loading. The controlling of the V_L was achieved by regulating the B_{SVC}. The function of SVC device was to maintain the reactive power in order to keep reactive power balance in power system networks. When the reactive power was controlled, the load voltage was kept on a setting value. The SVC hold the load voltage around the reference voltage (V_{ref}). Consequently, the SVC susceptance varied according to the power system network need, while the reactive power supplied/absorbed by the SVC varied according to the SVC susceptance. Meanwhile, the real power (load) was weakly connected to voltage control scheme. When the real load was changed to high level, load voltage changed in moderate mode. On the other hand, the real power was strongly connected to rotor angle (power angle) of control scheme point of view. Unfortunately, this topic is not discussed in this research.

The error percentage of the reference voltage and load voltage was used to validate the proposed controller. The error percentage was obtained from the reference voltage and load voltage difference. The formulation of the error percentage is represented in Eq.(21)

$$Err = \frac{\left|V_L - V_{ref}\right|}{V_{ref}} \times 100\% \cdots\cdots\cdots\cdots\cdots\cdots\cdots\cdots (21)$$

where Err, V_L and V_{ref} are the error percentage, load and reference voltage, respectively. The V_L is the observed value on

the load bus. From Table 4, the maximum Err in all cases for the λ_1 at the value of $j0.20$ pu was obtained at 0.14%. This maximum Err was sufficiently small. The results indicate that the proposed controller gave a good reactive power support to power system networks in order to control and maintain the load voltage magnitude.

5.4 Improvement of Transient Voltage Responses

The performances of respective controller were analyzed in transient voltage responses with additional three load types such as reactive, real and complex loads.

5.4.1 Transient voltage response with a LC-SVC

The transient voltage temporal responses of a LC-SVC are as follows: the V_{min} for an initial load ($\lambda_1 = j0.0$ pu) was obtained at the value of 0.9340 pu. Unfortunately, the V_{min} slightly decreased to 0.9326 pu when the λ_1 was increased to $j0.02$ pu. The V_{min} would continually decrease when the λ_1 was increased. The V_{min} achieved the minimum value at 0.9119 pu for the λ_1 at $j0.20$ pu. The V_{min} of the λ_2 for the values of 0.02 – 0.22 pu slightly increased from values of 0.9441 to 0.9464 pu. In addition, the V_{min} also slightly decreased from values of 0.9450 to 0.9406 pu when the λ_3 was increased from $0.02 + j0.02$ to $0.17 + j0.17$ pu, respectively. The load voltage responses were rather oscillated in a long time. Moreover, the t_{st} for the λ_1, λ_2 and λ_3 were achieved at times of 16, 18 and 18 s, respectively.

5.4.2 Transient voltage response with an ANFIS-based CC-SVC

The simulation results of the ANFIS-based CC-SVC are obtained as follows: The V_{min} for the λ_1 at an initial value was at the value of 0.9207 pu. The V_{min} slightly decreased when the λ_1 was increased again. The V_{min} was achieved at minimum value ($V_{min} = 0.8785$ pu) for the λ_1 maximum at $j0.20$ pu. The V_{min} for the λ_2 in a range of 0.02 to 0.22 pu was obtained at the values of 0.9441 to 0.9440 pu. The V_{min} for the λ_3 at $(0.02 + j0.02)$ to $(0.17 + j0.17)$ pu slightly decreased reaching the values of 0.9485 to 0.9394 pu, respectively.

Furthermore, the t_{min} for the λ_1, λ_2 and λ_3 occurred at around times of 0.59 to 0.92, 0.59 to 0.57 and 0.67 to 0.52 s, respectively. The t_{st} for the λ_1, λ_2 and λ_3 were achieved at the times of 11.05 to 13.11, 17.10 to 17.12 and 16.94 to 17.02 s, respectively. By comparing the t_{st}, it can be inferred that the ANFIS-based CC-SVC t_{st} exhibited shorter settling time than that of a LC-SVC. Meanwhile, the V_{min} for the ANFIS-based CC-SVC was lower than that of the LC-SVC (Fig. 9).

5.4.3 Improvement of transient voltage response with a proposed controller

The transient voltage response was improved significantly when the proposed controller was applied to power systems. Figure 9 shows the performance of the proposed controller for an additional reactive load at the value of $j0.12$ pu. It can be seen from the Fig. 9 and Table 5, the minimum voltages (V_{min}) for the LC-SVC, ANFIS-based CC-SVC and proposed controller were achieved at the values of 0.9246, 0.9362 and 0.9435 pu, respectively. Based on this simulation results, the proposed controller achieved the highest value of minimum voltage ($V_{min} = 0.9435$ pu), while, the t_{min} for the LC-SVC, ANFIS-based CC-SVC and proposed controller were achieved at times of 0.63, 0.69 and 0.39 s. And the t_{st} were achieved at times of 16.27, 12.05 and 7.01 s, respectively.

From the settling time point of view, it appears that the proposed controller made the power systems quickly reach the equilibrium point (steady state). The V_L oscillated only in 3 cycles, this oscillation quickly damped to the equilibrium point to 0.98 pu. On the contrary, the V_L of other controllers oscillated in 5 cycles. The performances of respective controllers were known from their temporal responses. It is shown that the proposed controller gave better performance than the others because the shortest settling time was obtained by this controller at 7.01 s. This happened because controller parameters such as linear gain, nonlinear gain and PID gain simultaneously well tuned. But, due to not having nonlinear gain and PID gain, their parameter settings were very limited.

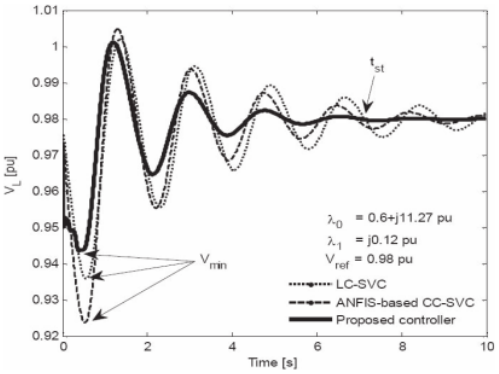

Fig. 9. Improvement of transient voltage response when the λ_1 was forced to load bus

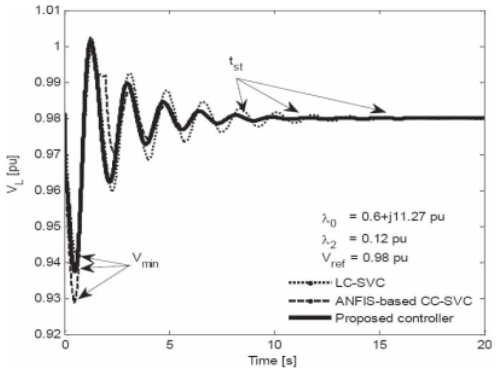

Fig. 10. Improvement of the transient voltage response when the λ_2 at the value of 0.12 pu

The improvement of the transient V_L response at an additional real load at 0.12 pu is shown in Fig. 10. In this scenario, the settling times for the LC-SVC, ANFIS-based CC-SVC and proposed controller were achieved at 18.11, 17.16 and 10.11 s, respectively. The proposed controller had the shortest settling time when compared with other methods. Meanwhile, the minimum voltage for the LC-SVC, ANFIS-based CC-SVC and proposed controller had a little deviation at the values of 0.9453, 0.9441 and 0.9374 pu, respectively. The LC-SVC had the highest V_{min} compared to

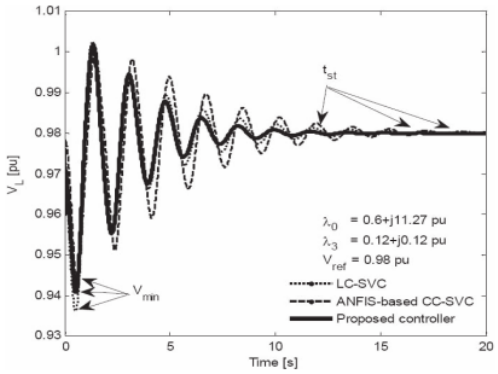

Fig. 11. Improvement of the transient voltage response when the $\lambda_3 = 0.12 + j0.12$ pu was forced to load bus

other methods. The minimum voltage of the ANFIS-based CC-SVC and proposed controller decreased in this simulation caused by effect of additional gains such as: Nonlinear, proportional, integral and differential controller gains. The respective controller gains for the nonlinear, proportional, integral and differential gains were set at the values of 0.08, 2.1995×10^{-2}, 3.9439×10^{-4} and 8.3×10^{-3}, respectively. The V_L temporal responses of 3 controllers for λ_3 at the value of $0.12 + j0.12$ pu are shown in Fig. 11. It indicates that the transient voltage was significantly improved when the proposed controller was applied to power systems. The settling times for the LC-SVC, ANFIS-based CC-SVC and proposed controller were achieved at the times of 18.16, 17.02 and 11.70 s, respectively. Again, this result proved that the proposed controller provided the shortest settling time. The minimum voltages for the LC-SVC, ANFIS-based CC-SVC and proposed controller were reached at the values of 0.9413, 0.9441 and 0.9407 pu, respectively.

Simulation results of the proposed controller showed better performance in both transient and steady states than the others. For instance, the transient load voltage dynamics were significantly improved using an additional PID-loop, indicated by the increase of minimum voltage and decrease of settling time. The overall results show that our proposed controller achieved more significant improvement than that of the previous methods.

6. Conclusion and Future Works

Chaotic oscillation, voltage collapse phenomena and their effects on critical loading of power system operation were deeply investigated in this research. The ANFIS-based CC-SVC with an additional PID-loop controller was proposed to suppress chaos and voltage collapse in power systems. Moreover, this type of controller was able to improve the transient load voltage responses. The results show that the effectiveness of the proposed controller to improve the load voltage transient response for the minimum voltage and settling time was achieved at the values of 0.9435 pu and 7.01 s, respectively. It shows that from the experimental result, the proposed method gave better performance than the others. In addition, this proposed controller was able to improve stability degree of power systems. The load voltage improvement was done by adjusting the reactive power supplied by the SVC device. When the reactive load was increased, the SVC susceptance and the reactive power supplied by the SVC had to be increased also in order to maintain reactive power balance in power system operation.

In the future, intelligent techniques based particle swarm optimization (PSO) will be utilized to optimize the control parameters. It is expected that heavy computation time can be reduced and the settling time can be suppressed significantly.

References

(1) H.-D. Chiang, I. Dobson, R.J. Thomas, J.S. Thorp, and L.F. Ahmed: "On Voltage Collapse in Electric Power Systems", *IEEE Trans. Power Syst.*, Vol.5, No.2, pp.601–611 (1990)

(2) L.F. Mello, A.C.Z. de Sauza, G.H. Yoshinory, Jr., and C.V. Schneider: Voltage Collapse in Power Systems: Dynamical Studies from a Static Formulation, Math. Problem in Engineering, Hindawi Pub. Corp. (2006)

(3) H.-D. Chiang, P.P. Varaiya, F.F. Wu, and M.G. Lauby: "Chaos in a Simple Power System", *IEEE Trans. Power Syst.*, Vol.8, No.4 (1993)

(4) H.O. Wang: "Control of Bifurcation and Routes to Chaos in Dynamical System", Thesis Report Ph. D, Institute for Systems Research, The University of Maryland, USA (1993)

(5) H.O. Wang, E.H. Abed, and A.M.A. Hamdan: "Bifurcations, Chaos, and Crises in Voltage Collapse of a Model Power System", *IEEE Trans. CAS* 1: Fundamental, Theory and Applications, Vol.41, No.3 (1994)

(6) H.-D. Chiang, (Eds.) G. Chen, D.J. Hill, and X. Yu: "Application of Bifurcation Analysis to Power Systems", in Bifurcation Control: Theory and Applications, pp.1–28, Springer-Verlag, Germany (2003)

(7) I. Dobson, (Eds.) G. Chen, D.J. Hill, and X. Yu: "Distance to Bifurcation in Multidimensional Parameter Space: Margin Sensitivity and Closest Bifurcation", in Bifurcation Control: Theory and Applications, pp.49–66, Springer-Verlag, Germany (2003)

(8) Y. Yu, H. Jia, P. Li, and J. Su "Power System Instability and Chaos", Proc. of the 14th PSCC, Sevilla (2002)

(9) Y. Yu, H. Jia, P. Li, and J. Su: "Power System Instability and Chaos", *Elect. Power Syst. Res.*, Vol.65, pp.187–195 (2003)

(10) K.G. Rajesh and K.R. Padiyar: "Bifurcation Analysis of a Three Node Power System with Detailed Models", *Elect. Power & Energy Syst.*, Vol.21, pp.375–393 (1999)

(11) I M. Ginarsa, A. Soeprijanto, and M.H. Purnomo: "Implementation of Classical Model to Chaotic Identification in Power Systems due to Disturbing of Energy", Proc. of the 9th SITIA Surabaya (2008) (in Indonesian)

(12) I M. Ginarsa, A. Soeprijanto, and M.H. Purnomo: "Modelling of Chaotic Behavior in Power Systems Using Recurrent Neural Networks", Proc. of ICA-CIA, pp.51–55, Jakarta (2008)

(13) T.S. Parker and L.O. Chua: Chaos: A Tutorial for Engineers, invited paper, *Proc. IEEE*, Vol.75, No.8, pp.982–1008 (1987)

(14) G. Chen: "Chaos: Control and Anti-control", *IEEE Circuits & Syst. Soc. Newsletter*, Vol.9, No.1 (1998)

(15) Z.-M. Lei, Z.-J. Liu, H.-X. Sun, and H.-X. Liu: "Control and Application of Chaos in Electrical System", Proc.of the 4th Int. Conf. Machine Learning and Cybernatics, Guangzhou (2005)

(16) K. Konishi and H. Kokame: "Stabilizing and Tracking Chaotic Orbits Using a Neural Network", Proc. NOLTA'95, Las Vegas, USA (1995)

(17) R.E. Precup, M.L. Marius, and S. Preitl: "Lorenz Stabilization Using Fuzzy Controller", *Int. J. Comp., Comm. & Control*, Vol.II, No.3 (2007)

(18) O. Calvo and J.H.E. Cartwright: "Fuzzy Control of Chaos", *Int. J. Bifurcation & Chaos*, Vol.8, pp. 1743–1747 (1998)

(19) M. Dhamala, Y.-C. Lai, and E.J. Kostelich: "Analyses of Transient Chaotic Time-series", *Phys. Rev. E*, Vol.64 (2001)

(20) M. Dhamala and Y.-C. Lai: "Controlling Transient Chaos in Deterministic Flows with Applications to Electric Power Systems and Ecology", *Phys. Rev. E*, Vol.59, No.2, pp.1646–1655 (1999)

(21) J. Krishnaiah, C.S. Kumar, and M.A. Faruqi: "Modeling and Control of Chaotic Processes through Their Bifurcation Diagrams Generated with the Help of Recurrent Neural Network Models: Part 1-Simulation Studies", *J. Process Control*, Vol.16, pp.53–66, Elsevier (2006)

(22) I M. Ginarsa, A. Soeprijanto, and M.H. Purnomo: "Controlling Chaos and Voltage Collapse Using Nonlinear Autoregressive Moving Average-Neural Networks (NARMA-NN) in Power Systems", Jurnal Ilmu Dasar, University of Jember, Indonesia (in press) (In Indonesian)

(23) J. Zhang, J.Y. Wen, S.J. Cheng, and J. Ma: "A Novel SVC Allocation Method for Power System Voltage Stability Enhancement by Normal Forms of Diffeomorphism", *IEEE Trans. Power Syst*., Vol.22, No.4 (2007)

(24) R. Minguez, F. Milano, R.Z. Minano, and A.J. Conejo: "Optimal Network Placement of SVC Devices", *IEEE Trans. Power Syst*., Vol.22, No.4 (2007)

(25) J.G. Singh, S.N. Singh, and S.C. Srivastava: "An Approach for Optimal Placement of Static VAR Compensators Based on Reactive Power Spot Price", *IEEE Trans. Power Syst*., Vol.22, No.4 (2007)

(26) M.M. Farsangi, H.H. Pour, Y.-H. Song, and K.Y. Lee: "Placement of SVCs and Selection of Stabilizing Signals in Power Systems", *IEEE Trans. Power Syst*., Vol.22, No.3 (2007)

(27) A. Soeprijanto, N. Yorino, and H. Sasaki: "Design of Robust Coordinated SVC Supplementary Controllers", *Elect. Power Syst. Res*., Vol.58, pp.141–148 (2001)

(28) M.S. Ballal, Z.J. Khan, H.M. Suryawanshi, and R.L. Sonolikar: "Adaptive Neuro-fuzzy Inference System for the Detection of Inter-turn Insulation and Bearing Wear Faults in Induction Motor", *IEEE Trans. Industrial Electronics*, Vol.54, No.1, pp.250–258 (2008)

(29) M. Sobha, R.S. Kumar, and S. George: "ANFIS Based Supplementary Controller for Damping Low Frequency Oscillations in Power Systems", JES on-line, http://journal.esrgroups.org/jes/ (2007)

(30) P. Mitra, S. Malik, S.P. Chowdhury, and S.P. Chowdhury: "ANFIS Based Automatic Voltage Regulator with Hybrid Learning Algorithm", *Int. J. Innov. in Energy Syst. & Power* (2008)

(31) I M. Ginarsa, A. Soeprijanto, and M.H. Purnomo: "Controlling Chaos Using ANFIS-based Composite Controller (ANFIS-CC) in Power Systems", Proc. of ICICI-BME 2009, pp.120–124, Bandung, Indonesia (2009)

(32) I M. Ginarsa, A. Soeprijanto, and M.H. Purnomo: "Controlling Chaos and Voltage Collapse Using an ANFIS-based Composite Controller-Static Var Compensator (CC-SVC) in Power Systems", *Int. J. Elect. Power & Energy Syst*., Elsevier (in review)

(33) Y.-T. Juang, Y.-T. Chang, and C.-P. Huang: "Design of Fuzzy PID Controllers Using Modified Triangular Membership Functions", *Information Sciences*, Vol.178, pp.1325–1333 (2008)

(34) J.-S. Chiou, and M.-T. Liu: "Numerical Simulation for Fuzzy-PID Controllers and Helping EP Reproduction with PSO Hybrid Optimization Algorithm", *Simulation Modelling Practice & Theory*, Vol.17, pp.1555–1565 (2009)

(35) V. Mukherjee and S.P. Ghoshal: "Intelligent Particle Swarm Optimized Fuzzy PID Controller for AVR System", *Elec. Power Syst. Res*., Vol.77, pp.1689–1698 (2008)

(36) I M. Ginarsa, A. Soeprijanto, M.H. Purnomo, Syafaruddin, and T. Hiyama: "Improvement of Transient Voltage Responses Using an Additional PID-loop on ANFIS-based Composite Controller-SVC (CC-SVC) to Control Chaos and Voltage Collapse in Power Systems", Proc. of The 5th ICAST Conference, Kumamoto University, Japan (2010)

(37) P. Kundur: Power System Stability and Control, EPRI, McGraw-Hill, New York (1994)

(38) K.T. Alligood, T.D. Sauer, and J.M. Yorke: Chaos: An Introduction to Dynamical Systems, Springer-Verlag, New York (2000)

(39) IEEE/PES: Voltage Stability Assessment, Procedure and Guides, Power System Stability Subcommittee, Special Publication, http://www.uwaterloo.ca (2000)

(40) X.-P. Zhang, C. Rehtanz, and B. Pal: Flexible AC Transmission Systems: Modelling and Control, Springer-Verlag, Berlin, Germany (2006)

(41) J.-S.R. Jang, C.T. Sun, and E. Mizutani: Neuro-fuzzy and soft computing: a Computational approach to learning and machine intelligence, Prentice-Hall International, Inc., USA (1997)

(42) —: MATLAB Version 7.6 (2008a): The Language of Technical Computing, The Matworks Inc, (2008)

I Made Ginarsa (Student Member) was born in Badung Regency, Bali, Indonesia, on March 25, 1970. He received B.Eng. and M.Eng. degrees in Elect. Eng. from Udayana (1997) and Gadjah Mada University (2001), respectively. He is pursuing a Ph.D. degree in Elect. Eng., ITS, Indonesia. Now, he is studying at Electric Power System Lab., Kumamoto University as a research student. His research interests are dynamic and voltage stability, nonlinear dynamic in power systems and neuro-fuzzy logic control application in power systems.

Adi Soeprijanto (Non-member) was born on April 5, 1964. He received MS and Ph.D. degrees in Electrical Engineering from Bandung Institute of Technology and Hiroshima University in 1995 and 2001, respectively. Since 2009, he has been a professor at the Department of Electrical Engineering, Institut Teknologi Sepuluh Nopember (ITS), Indonesia. His current research interests include the application of intelligent technology to power system operation, management and control. He is a member of the Indonesian Power System Expert Association (IATKI) of Indonesia.

Mauridhi Hery Purnomo (Non-member) received the B.S. degree in electrical engineering from Institut Teknologi Sepuluh Nopember (ITS) Indonesia, M.Eng. and Ph.D. degrees in Electrical Engineering from Osaka City University, Japan. He is a professor at Department of Electrical Engineering, ITS. He has involved in research and teaching in the field of intelligent systems, pattern recognition power system simulation and computer programming.

Syafaruddin (Non-member) received his B.Eng. degree in Electrical Engineering from Universitas Hasanuddin, Indonesia, in 1996, M.Eng degree in Electrical Engineering from University of Queensland, Australia, in 2004 and D.Eng. degree from Kumamoto University, Japan in 2009. He is currently working in Kumamoto University as a project assistant professor for Graduate School of Science and Technology. His research interests include distributed generation planning, maximum power point tracking control of photovoltaic system, power system real-time simulation and neuro-fuzzy logic control application in power systems.

Takashi Hiyama (Member) received his B.E., M.S. and Ph.D. degrees in Electrical Engineering from Kyoto University in 1969, 1971 and 1980, respectively. Since 1989, he has been a professor at the Department of Computer Science and Electrical Engineering, Kumamoto University, Japan. His current research interests include the intelligent system applications to power system operation, control and management. He is a senior member of IEEE, a member of IEEJ and Japan Solar Energy Society.

Improvement of Transient Voltage Responses using an Additional PID-loop on ANFIS-based Composite Controller-SVC (CC-SVC) to Control Chaos and Voltage Collapse in Power Systems

ORIGINALITY REPORT

12%	9%	8%	1%
SIMILARITY INDEX	INTERNET SOURCES	PUBLICATIONS	STUDENT PAPERS

PRIMARY SOURCES

1	iaescore.com Internet Source	2%
2	journal.uad.ac.id Internet Source	1%
3	Mohamed Nayel. "Investigation of Lightning Rod Shielding Angle", IEEJ Transactions on Power and Energy, 2011 Publication	1%
4	jpels.org Internet Source	1%
5	Mukherjee, V.. "Intelligent particle swarm optimized fuzzy PID controller for AVR system", Electric Power Systems Research, 200710 Publication	<1%
6	Yixin Yu, Hongjie Jia, Peng Li, Jifeng Su. "Power system instability and chaos", Electric Power	<1%

Systems Research, 2003
Publication

7	Hsiao-Dong Chiang, Chih-Wen Liu, P.P. Varaiya, F.F. Wu, M.G. Lauby. "Chaos in a simple power system", IEEE Transactions on Power Systems, 1993 Publication	<1 %
8	www.iaescore.com Internet Source	<1 %
9	eng.unhas.ac.id Internet Source	<1 %
10	www.gsst.kumamoto-u.ac.jp Internet Source	<1 %
11	P. Mitra, S. Maulik, S. P. Chowdhury, S. Chowdhury. "ANFIS based automatic voltage regulator with hybrid learning algorithm", 2007 42nd International Universities Power Engineering Conference, 2007 Publication	<1 %
12	internationalscienceindex.org Internet Source	<1 %
13	Dimas Anton Asfani, Syafaruddin, Mauridhi Heri Purnomo, Takashi Hiyama. "Temporary Short Circuit Detection in Induction Motor Winding Using Second Level Haar-Wavelet Transform", IEEJ Transactions on Industry Applications, 2011	<1 %

	Publication	
14	www.journal.uad.ac.id Internet Source	<1 %
15	Hongjie Jia, Yixin Yu, Peng Li, Jifeng Su. "Torus bifurcation and chaos in power systems", Proceedings. International Conference on Power System Technology, 2002 Publication	<1 %
16	Chin-Woo Tan, M. Varghese, P. Varaiya, F.F. Wu. "Bifurcation, chaos, and voltage collapse in power systems", Proceedings of the IEEE, 1995 Publication	<1 %
17	archive.org Internet Source	<1 %
18	ies.ieee-ies.org Internet Source	<1 %
19	www.ijert.org Internet Source	<1 %
20	H.-D. Chiang, I. Dobson, R.J. Thomas, J.S. Thorp, L. Fekih-Ahmed. "On voltage collapse in electric power systems", Conference Papers Power Industry Computer Application Conference, 1989 Publication	<1 %
21	acadpubl.eu Internet Source	

		<1%
22	core.ac.uk Internet Source	<1%
23	docplayer.net Internet Source	<1%
24	Submitted to The University of the South Pacific Student Paper	<1%
25	publik.tuwien.ac.at Internet Source	<1%
26	studylib.net Internet Source	<1%
27	H.-D. Chiang, I. Dobson, R.J. Thomas, J.S. Thorp, L. Fekih-Ahmed. "On voltage collapse in electric power systems", IEEE Transactions on Power Systems, 1990 Publication	<1%
28	Muthana T. Alrifai, Mohamed Zribi. "Sliding Mode Control of Chaos in a Single Machine Connected to an Infinite Bus Power System", Mathematical Problems in Engineering, 2018 Publication	<1%
29	waset.org Internet Source	<1%

30	www.nature.com Internet Source	<1 %
31	cogprints.org Internet Source	<1 %
32	dgjsxb.ces-transaction.com Internet Source	<1 %
33	digital-library.theiet.org Internet Source	<1 %
34	te.unram.ac.id Internet Source	<1 %
35	www.scribd.com Internet Source	<1 %
36	R. C. David, M.-B. Radac, S. Preitl, J. K. Tar. "Particle Swarm Optimization-based design of control systems with reduced sensitivity", 2009 5th International Symposium on Applied Computational Intelligence and Informatics, 2009 Publication	<1 %
37	doku.pub Internet Source	<1 %
38	espace.library.uq.edu.au Internet Source	<1 %
39	livrepository.liverpool.ac.uk Internet Source	<1 %

40	www.elec.osaka-sandai.ac.jp Internet Source	<1%
41	www.hindawi.com Internet Source	<1%
42	F. Liu, R. Yokoyama, Y. C. Zhou, M. Wu. "TCSC wide-area damping controller to enhance the damping of inter-area oscillation for power systems with considering the time delay of wide-area signals", 2010 International Conference on Power System Technology, 2010 Publication	<1%
43	GUANRONG CHEN, JORGE L. MOIOLA, HUA O. WANG. "BIFURCATION CONTROL: THEORIES, METHODS, AND APPLICATIONS", International Journal of Bifurcation and Chaos, 2012 Publication	<1%
44	Mark Gordon, David J. Hill. "Global transient stability and voltage regulation for multimachine power systems", 2008 IEEE Power and Energy Society General Meeting - Conversion and Delivery of Electrical Energy in the 21st Century, 2008 Publication	<1%
45	azadproject.ir Internet Source	<1%
	dr.ntu.edu.sg	

46	Internet Source	<1%
47	people.bath.ac.uk Internet Source	<1%
48	pt.scribd.com Internet Source	<1%
49	www.docme.ru Internet Source	<1%
50	www.gitam.edu Internet Source	<1%
51	www.scipub.org Internet Source	<1%
52	www.slideshare.net Internet Source	<1%
53	A. Matsushima. "Analysis of tropical attenuation statistics using synthetic storm for millimeter-wave wireless network design", 2008 5th IFIP International Conference on Wireless and Optical Communications Networks (WOCN 08), 05/2008 Publication	<1%

Exclude quotes	Off	Exclude matches	Off
Exclude bibliography	On		

Improvement of Transient Voltage Responses using an Additional PID-loop on ANFIS-based Composite Controller-SVC (CC-SVC) to Control Chaos and Voltage Collapse in Power Systems

GRADEMARK REPORT

FINAL GRADE

/0

GENERAL COMMENTS

Instructor

PAGE 1

PAGE 2

PAGE 3

PAGE 4

PAGE 5

PAGE 6

PAGE 7

PAGE 8

PAGE 9

PAGE 10

PAGE 11

PAGE 12

PAGE 13